Bone Reports 14 (2021) 100754

Contents lists available at ScienceDirect

Bone Reports

journal homepage: www.elsevier.com/locate/bonr

Spatial survey of non-collagenous proteins in mineralizing and non-mineralizing vertebrate tissues *ex vivo*

Putu Ustriyana [a,*,1], Fabian Schulte [b,c], Farai Gombedza [d], Ana Gil-Bona [b,c], Sailaja Paruchuri [d], Felicitas B. Bidlack [b,c], Markus Hardt [b,c], William J. Landis [a,1], Nita Sahai [a,e,f,**]

[a] *School of Polymer Science and Polymer Engineering, The University of Akron, Akron, OH 44325, USA*
[b] *The Forsyth Institute, Cambridge, MA 02142, USA*
[c] *Department of Developmental Biology, Harvard School of Dental Medicine, Boston, MA 02115, USA*
[d] *Department of Chemistry, The University of Akron, Akron, OH 44325, USA*
[e] *Department of Geosciences, The University of Akron, Akron, OH 44325, USA*
[f] *Integrated Bioscience Program, The University of Akron, Akron, OH 44325, USA*

ARTICLE INFO

Keywords:
Vertebrate
Mineralization
Type I collagen
Non-collagenous protein
Proteomics

ABSTRACT

Bone biomineralization is a complex process in which type I collagen and associated non-collagenous proteins (NCPs), including glycoproteins and proteoglycans, interact closely with inorganic calcium and phosphate ions to control the precipitation of nanosized, non-stoichiometric hydroxyapatite (HAP, idealized stoichiometry $Ca_{10}(PO_4)_6(OH)_2$) within the organic matrix of a tissue. The ability of certain vertebrate tissues to mineralize is critically related to several aspects of their function. The goal of this study was to identify specific NCPs in mineralizing and non-mineralizing tissues of two animal models, rat and turkey, and to determine whether some NCPs are unique to each type of tissue. The tissues investigated were rat femur (mineralizing) and tail tendon (non-mineralizing) and turkey leg tendon (having both mineralizing and non-mineralizing regions in the same individual specimen). An experimental approach *ex vivo* was designed for this investigation by combining sequential protein extraction with comprehensive protein mapping using proteomics and Western blotting. The extraction method enabled separation of various NCPs based on their association with either the extracellular organic collagenous matrix phases or the inorganic mineral phases of the tissues. The proteomics work generated a complete picture of NCPs in different tissues and animal species. Subsequently, Western blotting provided validation for some of the proteomics findings. The survey then yielded generalized results relevant to various protein families, rather than only individual NCPs. This study focused primarily on the NCPs belonging to the small leucine-rich proteoglycan (SLRP) family and the small integrin-binding ligand N-linked glycoproteins (SIBLINGs). SLRPs were found to be associated only with the collagenous matrix, a result suggesting that they are mainly involved in structural matrix organization and not in mineralization. SIBLINGs as well as matrix Gla (γ-carboxyglutamate) protein were strictly localized within the inorganic mineral phase of mineralizing tissues, a finding suggesting that their roles are limited to mineralization. The results from this study indicated that osteocalcin was closely involved in mineralization but did not preclude possible additional roles as a hormone. This report provides for the first time a spatial survey and comparison of NCPs from mineralizing and non-mineralizing tissues *ex vivo* and defines the proteome of turkey leg tendons as a model for vertebrate mineralization.

Abbreviations: B, rat bone; BSP, bone sialoprotein; DCN, decorin; E, EDTA extract; ECM, extracellular matrix; G, guanidine-HCl-only extract (for non-mineralizing tissues); G1, first guanidine-HCl extract; G2, second guanidine-HCl extract; Gla, gamma-carboxylated glutamic acid; MGP, matrix Gla protein; MT, turkey mineralizing tendon; NCP, non-collagenous protein; NMT, turkey never-mineralizing tendon; NT, turkey not-yet-mineralized tendon; OCN, osteocalcin; OPN, osteopontin; SIBLING, small integrin-binding ligand N-linked glycoprotein; SLRP, small leucine-rich proteoglycan; T, rat tail tendon; TLT, turkey leg tendon (gastrocnemius); TNAP, tissue-nonspecific alkaline phosphatase.

* Corresponding author.
** Correspondence to: N. Sahai, Department of Geosciences, The University of Akron, Akron, OH 44325, USA.
E-mail addresses: pu4@zips.uakron.edu (P. Ustriyana), sahai@uakron.edu (N. Sahai).
[1] Present address: Department of Preventive and Restorative Dental Sciences, School of Dentistry, University of California, San Francisco, San Francisco, CA 94143, USA.

https://doi.org/10.1016/j.bonr.2021.100754
Received 12 January 2021; Received in revised form 5 February 2021; Accepted 5 February 2021
Available online 10 February 2021

1. Introduction

Type I collagen accounts for the major portion of the extracellular matrix (ECM) in most mineralizing tissues of vertebrates (Weiner and Dove, 2003; George and Veis, 2008; Beniash, 2011; Nair et al., 2013). Non-collagenous proteins (NCPs), including glycoproteins and proteoglycans (PGs), are also present in the ECM of such tissues and it has been hypothesized that collagen in association with NCPs is important in regulating the mineralization process (Beniash, 2011). Similar to bone, vertebrate tendon is predominantly comprised of type I collagen (Aslan et al., 2008) with its matrix containing small amounts of NCPs (Kannus, 2000; Silver et al., 2001; Thorpe et al., 2013). Some tendons in certain avian species, such as turkeys, mineralize normally in their legs and wings (Landis, 1986; Landis and Song, 1991; Landis et al., 2002; Landis and Silver, 2002). Specific tendons in turkey legs have been previously used as models of vertebrate mineralization (Landis et al., 1993; Landis et al., 1996; Landis and Silver, 2002). These tendons, such as the gastrocnemius or Achilles tendon, mineralize along their length as the turkey matures. They do so in a progressive and sequential manner, which allows the deposition of mineral to be carefully followed both spatially and temporally. Thus, certain distal-to-proximal regions of these tissues may be identified by light and electron microscopy as respectively containing relatively older, more mature mineral; younger, less mature mineral; and no mineral. The latter regions will eventually mineralize with the age of the animal. Several features, such as type I collagen, specific NCPs, and apatite crystals formed in these tendons resemble those observed in bones (Berthet-Colominas et al., 1979; Landis and Silver, 2002). The presence of both mineralizing and non-mineralizing aspects in avian tendon tissue also provides a link between mineralization and distributions of NCPs.

Other vertebrate species have tendons that never mineralize, as for example, the rat tail tendon. Curiously, mineralization of rat tail tendon collagen differs when studied with calcium phosphate solutions *ex vivo* versus *in vitro*. Dissected tendon with its native arrangement of collagen fascicles does not mineralize *ex vivo*, whereas collagen fibrils extracted and reconstituted from the native tail tendon do mineralize (Glimcher et al., 1957; Zhang et al., 2003). Previous literature suggests that a loss of calcification inhibitors during the extraction and reconstitution procedure might be responsible for collagen mineralization observed *in vitro* (Glimcher, 2006). Thus, rat and turkey represent useful models to study regulation of tissue mineralization by NCPs, because rat bone and tail tendon, as well as mineralizing and non-mineralizing regions of turkey tendons, each consist of the same basic ECM proteins (largely type I collagen) but present different mineralization characteristics. The unique distribution of NCPs in each tissue could provide insights into the specific functions that NCPs may play in various mineralization stages.

Multiple studies have attempted to define functions of NCPs in bone mineralization *in vivo* and *in vitro* using different techniques but did not reach unequivocal conclusions (George and Veis, 2008). The described functional roles range from influencing bone cell activities to interacting directly with calcium and phosphate ions and minerals (Hunter et al., 1996; Murshed et al., 2004; George and Veis, 2008; O'Young et al., 2011). NCPs are commonly highly charged, being enriched in negatively charged amino acid residues. Several of these acidic NCPs belong to the family of small integrin-binding ligand N-linked glycoproteins (SIBLINGs) (George and Veis, 2008). The presence of negative charges on these proteins has been linked to their role in mediating biomineralization (Boskey, 1989; Ryuichi and Yoshinori, 1991; Gorski, 1992; Pampena et al., 2004; Staines et al., 2012). Specific mechanisms by which they regulate apatite formation in mineralized and non-mineralized tissues, however, remain elusive. Investigations of the localization of NCPs in mineralized tissue such as bone have principally concerned bone-related NCPs, whereas studies of non-mineralized tissues such as tendon have primarily focused on PGs (George and Veis, 2008; Thorpe et al., 2013). Some of the PGs investigated belong to the family of small leucine-rich proteoglycans (SLRPs), which are often associated with type I collagen in both bone and tendon (Schaefer and Iozzo, 2008; Chen and Birk, 2013). Studies *in vitro* have reported inconsistent roles for NCPs even when conducted on identical NCPs (Weiner and Dove, 2003; George and Veis, 2008; Beniash, 2011). Similarly, studies *in vivo* using knockout models were unable to link specific NCPs directly to phenotypic changes in the skeletal tissues, a result suggesting redundancy in the function of NCPs (Ducy et al., 1996; Boskey et al., 1998; Rittling and Feng, 1998; Holm et al., 2015). Altogether, it is challenging to draw firm conclusions as to the roles of specific NCPs from different studies because of the varying model systems, experimental protocols, and methodologies that were employed.

The main aim of the present investigation was to identify and compare NCPs that are present in mineralizing and non-mineralizing tissues from two male animal models, rat and turkey, to determine whether certain NCPs are unique to each tissue. This study also spatially localizes these NCPs to either non-mineralizing or mineralizing regions of the tissues, and more specifically to the organic matrix or the mineral phases of these regions. Our experimental approach utilized sequential extraction of NCPs followed by liquid chromatography-tandem mass spectroscopy (LC-MS/MS)-based proteomics analyses and validation by Western blotting. Sequential extraction permitted the identification of NCPs that might be strictly associated with the mineral phase, either within or on the surface of minerals, or with the principally collagenous matrix phase of the respective tissues. Alternatively, some NCPs may be associated with both mineral and organic matrix phases. Importantly, our analyses yielded a qualitative and quantitative (relative) comparison of various NCP families in the inorganic and organic phases of the tissues, instead of being limited only to individual NCPs. This work also provided, for the first time, a survey of proteins in turkey leg tendons (TLTs) that can serve as a model for vertebrate mineralization. For the purposes of this study, it must be noted that rat bone (B) and the mineralizing aspect of TLT (MT) are referred to as mineralizing tissues; the rat tail tendon (T), the not-yet-mineralized portion of TLT (NT), and the never-mineralizing aspect of TLT (NMT) are referred to as non-mineralizing tissues.

2. Experimental section

2.1. Tissue dissection and preparation

Ten-week-old normal male Sprague-Dawley rats ($n = 3$), weighing between 300 and 320 g, were purchased from Envigo (Indianapolis, IN). The animal protocol (#15-08-12-LRC) was approved by the Institutional Animal Care and Use Committee (IACUC) at The University of Akron (Akron, OH). Rat femurs and tail tendon were dissected after euthanasia (Fig. 1a and b). The femoral epiphyseal regions were removed and discarded. The resulting bone midshafts were then cleaned of attached soft tissue, including the periosteum, by scraping the bone surfaces with a periosteal elevator. The bone marrow was removed by vacuum aspiration and flushing with cold 1× phosphate buffered saline (PBS; Sigma-Aldrich, Milwaukee, WI). The tendons were cleaned by immersing them in cold 1× PBS.

Sixteen-week-old male domestic turkeys ($n = 3$) were obtained from Brunty Farms (Akron, OH). The normally mineralizing gastrocnemius tendons were dissected from both legs (Fig. 1a). The muscles and soft tissues attached to the tendons were carefully removed (Landis, 1986). Mineralizing aspects of the gastrocnemius were dissected into specimens ~5 cm in length and were identified as the hard and inflexible tendon regions proximal to the bifurcation of this tissue into two separate branches (Fig. 1b). The not-yet-mineralized tendon (NT) aspects, which will eventually mineralize over time, were taken by dissecting the flexible tissue regions proximal to the mineralizing tendon (MT) portions. The tendons distal to the mineralizing tendons at the bifurcation point were dissected as well, and they were referred to as the never-mineralizing tendons (NMT, Fig. 1b). All dissected tendon tissues were then cleaned in a manner identical to that of the rat tissues described

above.

Cleaned and isolated tissues were placed in cold 1× PBS with protease inhibitors (PI) containing 0.05 M 6-aminohexanoic acid, 0.005 M benzamidine HCl, and 0.001 M phenylmethanesulfonyl fluoride (pH 7.2, Sigma-Aldrich) (Termine et al., 1980). To ensure complete removal of attached soft tissue and fascia, samples were sonicated at 4 °C for 1 h in PBS-PI solution with 5× solution changes. The tissue samples were then snap-frozen in liquid nitrogen prior to storage at −80 °C. All the above procedures were performed within 3–5 h after the death of the animals (Termine et al., 1980). Prior to NCP extraction, the frozen tissue samples were cut into ~1 cm blocks using bone-cutting forceps and then ground to a powder under liquid nitrogen using a cryogenic mill (Model 6870 Freezer/Mill, SPEX SamplePrep, Metuchen, NJ).

2.2. NCP extraction

NCP extraction was performed by different means for either the mineralizing or non-mineralizing tissues of rat and turkey. The following methods were applied to both proteomics and Western blotting samples unless otherwise specified. Tissues from both rat and turkey were partitioned for proteomics and Western blotting analyses. Ground samples of mineralizing tissue were extracted sequentially in three steps following previous protocols with certain modifications (Fig. 1c) (Termine et al., 1980; Domenicucci et al., 1988). The ratio of tissue powder to extracting solution was 50 mg/mL. For proteomics analysis, ground tissue samples were incubated with 1 U of chondroitinase ABC (from *Proteus vulgaris*, Sigma-Aldrich) for 6 h at 37 °C prior to protein extraction and 65 mM dithiothreitol was added to all extraction solutions. Tissue powder was first extracted with constant stirring at 4 °C for 72 h in an aqueous solution containing 4 M guanidine-HCl (Santa Cruz Biotechnology, Dallas, TX), 0.05 M Tris, and PI cocktail (cOmplete™, Mini, EDTA-free, Roche, Mannheim, Germany, pH 7.4). The extract was centrifuged at 3000 rpm for 30 min at 4 °C (Eppendorf Centrifuge, model 5810 R, Radnor, PA). The initial guanidine extraction was used to dissociate NCPs from unmineralized matrix and cellular compartments such as osteocytes or tenocytes (George and Veis, 2008; Huang et al., 2008). The supernatant of this initial guanidine (G) extraction was designated as G1-B extract for rat bone (B) or G1-MT for mineralizing TLT (MT) samples (Fig. 1c-1).

The pellet remaining after the initial extraction and centrifugation was extracted for a second time using a solution containing 0.5 M EDTA, 0.05 M Tris, and PI cocktail (pH 7.4) with constant stirring for 72 h at 4 °C. EDTA was used to chelate Ca^{2+} and demineralize the tissue powder samples. This step was performed in order to extract NCPs that were bound to apatite crystals or occluded within the mineralized phase (Domenicucci et al., 1988; George and Veis, 2008; Huang et al., 2008). The supernatant of this EDTA (E) extraction was designated as the E-B or E-MT extract for rat bone and the mineralizing aspect of TLT, respectively (Fig. 1c-2).

A final (third) extraction was performed using the same procedures as those in the first extraction step. This final extraction was designed to reveal NCPs that were bound tightly to any non-extractable tissue matrix (organic phase) and exposed after demineralization (Domenicucci et al., 1988; George and Veis, 2008; Huang et al., 2008). The extracts from this

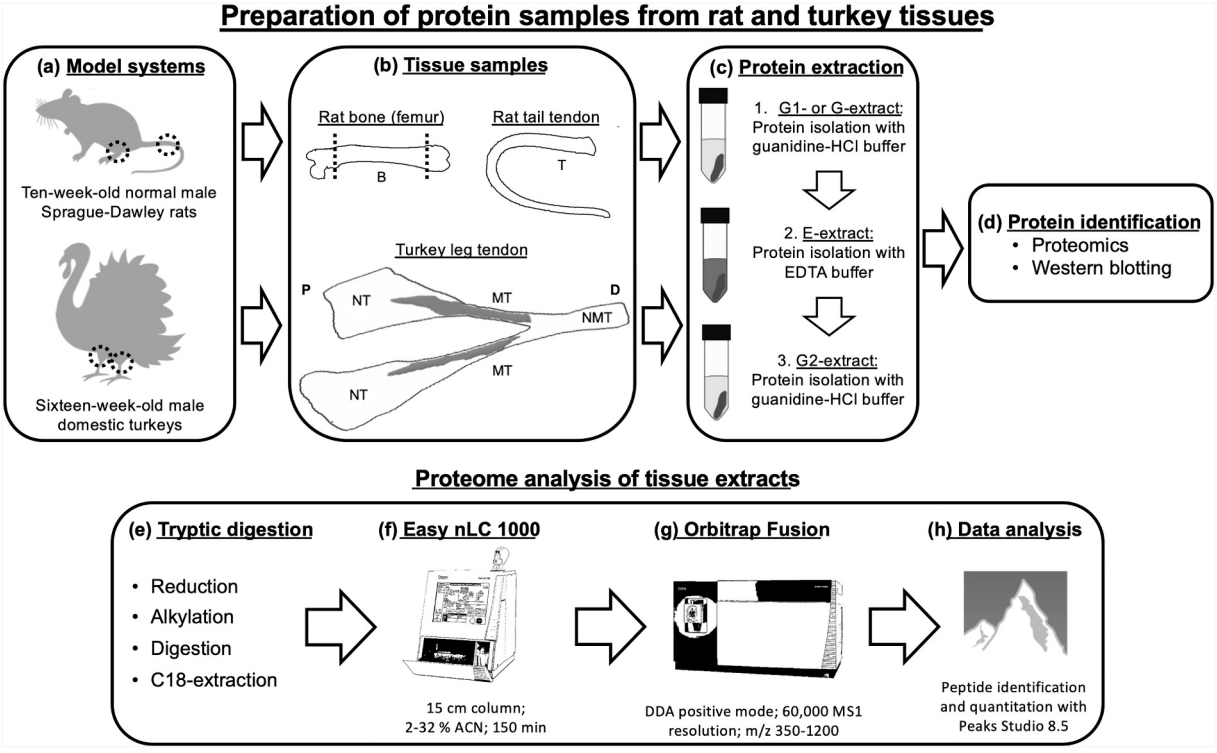

Fig. 1. Schematic diagram of protein extraction and proteome analysis procedures for rat and turkey mineralizing and non-mineralizing tissues. To study the protein inventory, tissues were isolated from ten-week-old normal male Sprague-Dawley rats and sixteen-week-old male domestic turkeys (a). The femoral bone (B) and tail tendon (T) were dissected from rats. The dissected leg tendons of turkey were divided into three regions: a mineralizing (MT) region, a region that has not-yet-mineralized (NT) at the time the turkey was sacrificed, and a never-mineralizing region (NMT) (b). These tissue sections were then pulverized prior to the protein extraction procedure. Sequential extraction steps for mineralizing tissues consisted initially of guanidine-HCl, followed by EDTA, and subsequently a second guanidine-HCl treatment yielding the protein extracts G1, E, and G2, respectively. The non-mineralizing tissues were extracted using only guanidine-HCl (G) (c). Proteins were then identified by proteomics and Western blotting (d). After each treatment, the protein extracts were tryptically digested (e) and the resulting peptides separated by nanoLC hyphenated to an Orbitrap Fusion mass spectrometer and analyzed by tandem mass spectrometry (MS/MS) (f, g). Proteins were identified and quantified through a label-free approach using the PEAKS Studio 8.5 software platform (h). P: proximal; D: distal; ACN: acetonitrile; DDA: data-dependent acquisition.

procedure were referred to as G2-B or G2-MT (Fig. 1c-3).

The non-mineralizing tendon tissues of the rat tail and the not-yet-mineralized and never-mineralizing aspects of TLT are comprised of only organic matrix; hence, they required no demineralization and EDTA extraction. In preliminary experiments we confirmed that G2-extracts of non-mineralizing tissues resulted in very low protein concentrations (data not shown) consistent with the notion that NCPs would have been extracted in the first guanidine extraction step. Accordingly, ground non-mineralizing tendon samples were extracted in solutions containing 4 M guanidine-HCl, 0.05 Tris, and PI (pH 7.4) with the same tissue powder-to-solution ratio (50 mg/mL) as the mineralizing tissues and conducted with constant stirring at 4 °C for 72 h. Extracts were centrifuged at 15,000*g* for 30 min at 4 °C (Avanti™ J-E Centrifuge, Beckman Coulter, Radnor, PA). The extracts obtained from this procedure were designated as G-T, G-NT, or G-NMT for rat tail tendon, the not-yet-mineralized TLT, or the never-mineralizing TLT samples, respectively.

After each extraction procedure, both bone and tendon extracts were concentrated by ultrafiltration (Amicon® Ultra-15 Centrifugal Devices, EMD Millipore, Taunton, MA) with a membrane molecular weight cut-off of 3 kDa. The cut-off was chosen after considering that the lowest molecular weight of the NCP of interest was ~5.7 kDa for osteocalcin. The filtrate was centrifuged at 5000*g* at 4 °C. Extracts were concentrated until the minimum desired total protein concentration was obtained (1.67 μg/μL). Protein concentrations were determined (in biological replicates) using Bicinchoninic acid (BCA) and Bradford assays (Pierce® BCA Protein and Coomassie Plus™ Bradford Assay Kit, Thermo Fisher Scientific, Waltham, MA). Protein extracts with guanidine were quantitated using the BCA assay while extracts with EDTA were quantitated using the Bradford assay as EDTA interferes with the BCA assay.

For proteomics analyses, 80 μg of extracted proteins were first digested by the addition of 1 μg trypsin (sequencing grade modified, Promega, Madison, WI) in 50 mM ammonium bicarbonate buffer and incubation at 37 °C overnight. An additional bolus of 1 μg trypsin was added to the extracts on the following day with incubation at 37 °C for 2 h. Digestions were stopped by the addition of 5 μL 10% trifluoroacetic acid (TFA), and the digests were desalted using Pierce C18 tips (Thermo Fisher Scientific) as described by the manufacturer and resuspended in 25 μL 0.1% formic acid after solvent evaporation in a SpeedVac (Eppendorf AG, Hamburg, Germany) (Fig. 1e). For normalization, 1 μL of custom iRT peptide standards (final concentration 50 nM) was added to each sample for retention time alignment.

2.3. nanoLC-MS/MS analysis

LC-MS/MS in data-dependent acquisition (DDA) mode was performed on an Easy-nLC 1000 system hyphenated to an Orbitrap Fusion mass spectrometer equipped with an Easy Spray ESI source (Thermo Fisher Scientific) (Fig. 1f and g). An Acclaim PepMap 100 (100 μm × 2 cm) trap column in conjunction with a PepMap RSLC C18 (ES801A, 75 μm × 15 cm, 100 Å particle size) column (Thermo Fisher Scientific) was employed for separation of tryptic peptides. Injection volumes were 5 μL. Mobile phase solution A was composed of 0.1% (v/v) formic acid in water and mobile phase solution B was composed of acetonitrile and 0.1% (v/v) formic acid. The flow rate was 300 nL/min and the column was heated to 45 °C. After 2 min at 2% solvent B, analytes were separated by a linear gradient up to 32% solvent B over 150 min. The column was subsequentially washed for 30 min at 2% and 98% solvent B using a saw-tooth gradient. The ion source temperature was maintained at 275 °C with a voltage of 1800 V in positive mode. Analytes were measured with a resolution of 60,000 in DDA mode in the scan range m/z 350–1200 with an automatic gain control (AGC) target of 3.0×10^5 ion counts and an injection time of 250 ms. The MS/MS analyses were carried out by selecting the 20 most abundant precursor ions (intensity $\geq 2.0 \times 10^4$ ions) in the quadrupole mass analyzer over a 2.5 Da m/z isolation window and fragmented by higher energy collisional dissociation with a normalized collision energy of 30. Fragment ions were detected in the Orbitrap mass analyzer at 15,000 resolution with an AGC target setting of 5×10^4 and a maximum ion accumulation time of 150 ms. The dynamic exclusion time for previously analyzed precursor ions and isotopes was 40 s.

2.4. Proteome identification

Protein identification and label-free quantification were performed using the PEAKS Studio 8.5 software suite (Fig. 1h). The raw data were refined utilizing merge scans with the following parameters: retention time window 10 min, precursor m/z tolerance 10 ppm, and precursor mass and charge states $z = 1$–10. Other data pre-processing (centroiding, deisotoping, and deconvolution) was executed automatically. Proteins were identified by searching against the UniProt database for *Rattus norvegicus* (for rat samples; $n = 2$) and the RefSeq database for *Meleagris gallopavo* (for turkey samples ($n = 2$) downloaded September 23, 2019) with the following search parameters: parent mass error tolerance 10 ppm; fragment mass error tolerance 0.05 Da; trypsin enzyme specificity (K,R) with cleavage prior to proline permitted; variable modifications: phosphorylation (STY), pyro-glu (Q), oxidation (M), deamidation (NQ), carboxylation (E); and one non-specific cleavage specificity on one terminus, maximal two missed cleavages, maximal three variable post-translational modifications per peptide. The false discovery rate for identifications was determined using the decoy-fusion approach (Zhang et al., 2012). All peptides with a false discovery rate of ≤1% and proteins above the significance threshold of 20 (−10 lgP) were considered as identified. Two unique peptides were required for protein identification. Protein quantitation was conducted using the Top3 approach (Silva et al., 2006), where the peak areas of up to the three most abundant, unique peptides were utilized. Raw protein peak areas were exported as a CSV table and analyzed by using Microsoft Excel. Relative protein abundances were obtained by normalizing the peak area of each identified protein to the total protein peak area in each extract.

Gene Ontology (GO) classification enrichment analyses were conducted using the DAVID Bioinformatics Resources 6.8 online (https://david.ncifcrf.gov/tools.jsp) with default stringency criteria. The complete proteomes of *Rattus norvegicus* and *Meleagris gallopavo* were employed as reference databases for the respective rat and turkey. The enrichment analyses were conducted for all identified proteins in both rat and turkey.

2.5. Western blotting

Western blotting ($n = 3$) was conducted following a Bio-Rad (Richmond, CA) protocol with modifications (Duah et al., 2013). Briefly, extract samples were diluted in sample buffer to a final protein concentration of 1.25 μg/μL. After denaturation, the samples were centrifuged at 12000*g* for 15 min at 20 °C to separate insoluble particles. Depending on the NCP, different quantities of sample were loaded onto gels. For decorin and bone sialoprotein, 16.25 and 10 μg of rat and turkey samples were loaded, respectively. For identifying osteopontin, osteocalcin, and tissue-nonspecific alkaline phosphatase, 12.5 μg of each sample were loaded. The samples were subjected to 4–15% SDS-PAGE and transferred to PVDF membranes. Membranes were incubated with respective primary antibodies diluted in 1× TBS, 5% dry milk, and 0.1% Tween-20 overnight at 4 °C, and then they were incubated for 1 h with secondary antibody (1:5000).

Antibodies used were rabbit polyclonal antibody against murine decorin (LF-114), mouse osteopontin (LF-175), and rat bone sialoprotein (LF-87), kindly provided by Dr. Larry W. Fisher (NIDCR/NIH, Bethesda, MD), as well as rabbit polyclonal antibody against chicken osteopontin and bone sialoprotein, generously donated by Dr. Marc D. McKee (McGill University, Montreal, QC). Rabbit polyclonal antibody against human osteocalcin (sc-30044) and mouse monoclonal antibody against human tissue-nonspecific alkaline phosphatase (sc-137213) were

purchased from Santa Cruz Biotechnology. Dilution of the antibodies was as follows: 1:1250 for decorin, 1:1500 and 1:5000 for rat and turkey osteopontin and bone sialoprotein, respectively, and 1:500 for osteocalcin and tissue-nonspecific alkaline phosphatase. Secondary antibody used was peroxidase-conjugated donkey anti-rabbit or goat anti-mouse IgG (1:5000, Jackson ImmunoResearch Laboratories, Inc., West Grove, PA). The blots were then developed using Amersham ECL detection reagent (GE Healthcare, Buckinghamshire, UK) and imaged with a FluorChem E System (ProteinSimple, San Jose, CA).

3. Results and discussion

Termine et al. first developed a sequential protein extraction method for vertebrate mineralized tissues by treating tooth enamel initially with 4 M guanidine-HCl followed by demineralization (dissolution of hydroxyapatite, HAP) using EDTA/guanidine-HCl (Termine et al., 1980). The initial guanidine-HCl treatment dissociated cellular compartments including matrix and cells (osteoid and osteocytes, for example), blood, adhering connective tissues and accessible proteins that were not bound to the mineral phase. The second EDTA/guanidine-HCl treatment extracted proteins that were embedded in the mineralized phase of the tissues and tightly bound to the surface of apatite crystals (Termine et al., 1980; Fisher et al., 1987; George and Veis, 2008). Domenicucci et al. modified the Termine method by solely using EDTA for the second extraction and adding another guanidine-HCl treatment after demineralization (Domenicucci et al., 1988). This last extraction step removed tightly bound mineral-protected NCPs from other NCPs bound to the structural organic matrix of the tissues (Domenicucci et al., 1988; George and Veis, 2008). In the present study, we used this procedure to extract mineralizing tissues sequentially with guanidine-HCl (G1), EDTA (E), and guanidine-HCl (G2), whereas the non-mineralizing tissues were extracted using only guanidine-HCl (G) (Fig. 1c). The total protein concentration of each extract is listed in Table 1.

Upon protein extraction, proteomics was comprehensively used to determine the spatial localization of NCPs in the different phases of the ECM of the rat and turkey tissues of interest. Ninety proteins were cumulatively identified in the rat and 201 in the turkey tissue samples. In rat, most proteins were identified in the G1-extract of the mineralizing tissue and a similar trend was observed in turkey, as represented in Venn diagrams (Fig. 2). Of the proteins detected in rat and turkey, 96% and 86%, respectively, had GO annotations. GO analyses of the rat proteomes revealed that the ECM cluster (GO:0031012) was the most significantly enriched cellular component annotation term (p-value = 6.60×10^{-30}). The twenty-eight ECM-annotated proteins for rat are listed in Table 2. In turkey, sixteen proteins were annotated as ECM components (Table 3). The cellular component term most highly enriched (p-value = 2.5×10^{-39}) in turkey protein annotations was extracellular exosome (GO:0070062). Many of the proteins belonging to the ECM cluster are collagen chain proteins and PGs that are SLRP family members. Collagen proteins are known to comprise the structural proteinaceous matrix of bone and tendon (Weiner and Dove, 2003; George and Veis, 2008; Beniash, 2011; Nair et al., 2013), and SLRPs are ubiquitous proteins linked to collagens in bone and tendon (Schaefer and Iozzo, 2008; Chen and Birk, 2013). These PGs participate closely in the formation and organization of the collagenous matrix (Schaefer and Iozzo, 2008; Chen and Birk, 2013).

SLRPs possess multivalent binding abilities that can modulate the assembly and organization of the collagenous matrix in connective tissues. Of the seventeen known SLRPs (Schaefer and Iozzo, 2008; Chen and Birk, 2013), we identified nine in the current proteomics study (Fig. 3a (rat) and b (turkey)). Four of these proteins were localized to both rat and turkey: decorin (DCN), asporin (ASPN), fibromodulin (FMOD), and osteoglycin/mimecan (OGN). Biglycan (BGN) and keratocan (KERA) were exclusively found in rat, while chondroadherin (CHAD), lumican (LUM), and osteomodulin/osteoadherin (OMD) were identified only in turkey. Most of the SLRPs were found in relatively high abundance in the non-mineralizing tendon regions and only in G1- or G2-extracts of mineralizing tissues, results that suggest their exclusive association with the collagenous matrix or with cellular components of the tissues. Consistent with this notion, SLRP proteins were sparsely detected in the E-extracts of the mineralizing tissues of interest. The absence of SLRPs in the mineral phase provides evidence that this NCP family may not play a role in mineralization *in vivo*.

Among the SLRPs, DCN is the most abundant PG in bone and therefore has previously been considered to be a major factor in biomineralization (Fisher et al., 1983; Bianco et al., 1990). In tendon, previous studies have shown that DCN accounts for 80% of the total PG content in this tissue and is reported to be located between tendon collagen fibrils, fibers, and fascicles (Scott, 1996; Thorpe et al., 2013). The present proteomics analyses showed that DCN was localized most prominently in non-mineralizing tissues of both rat (Fig. 3a) and turkey (Fig. 3b). In mineralizing tissues, DCN was only detected in G2-extracts. These results indicate that DCN is associated with the organic collagenous fibrils/matrix, but not the mineral phase. The presence of DCN in these tissues was supported by Western blotting (Fig. 3c). In mammals, DCN consists of a protein core designated as decoron that has molecular mass ~40 kDa and a single chondroitin or dermatan sulfate glycosaminoglycan chain (Fisher et al., 1983, 1987; Bianco et al., 1990; Orgel et al., 2009; Thorpe et al., 2013). DCN has been detected as a diffuse band between 69 and 200 kDa in the Western blot membrane (Ramamurthy et al., 1996) and is known to homodimerize (Scott et al., 2004; Orgel et al., 2009). In the present study, DCN appeared as diffuse bands at ~75 and ~150 kDa in all rat and turkey extracts except the G1-extract. Bands around ~150 kDa likely indicate the dimerization of decorin. Earlier studies have not resolved whether DCN is present as a monomer or dimer and how it may interact with collagen *in vivo*, but the current work suggests that both monomeric and dimeric DCN are present in the collagenous matrices of the tissues investigated (Scott et al., 2004; Orgel et al., 2009; Orgel et al., 2011).

The association of DCN with the collagenous matrix of both non-mineralizing and mineralizing tissues in both rat and turkey was expected as previous reports have localized DCN in type I collagen-enriched tissues across different species (Scott et al., 1981; Fisher et al., 1983, 1987; Bianco et al., 1990; Hoshi et al., 1999; Kuwabara et al., 2002). DCN has been proposed to play a role in the proper alignment and stabilization of collagen fibrils during fibrillogenesis (Scott, 1996; Danielson et al., 1997; Reed and Iozzo, 2002). With regard to mineralization, DCN has been hypothesized to be an inhibitor of the process (Scott et al., 1981; Scott and Orford, 1981; Hoshi et al., 1999). Previous investigations of rat tail tendon inferred that DCN may inhibit

Table 1
Total protein concentration of sequential extracts (μg/μL) from rat bone and tail tendon and different regions of turkey leg tendons.

Rat				Turkey leg tendon				
Bone (B)			Tendon (T)	Mineralizing (MT)			Not-yet-min (NT)	Never-min (NMT)
G1	E	G2	G	G1	E	G2	G	G
12.5 ± 0.37	2.48 ± 0.18	2.58 ± 0.48	9.07 ± 0.55	6.91 ± 0.08	3.31 ± 0.19	1.84 ± 0.10	3.33 ± 0.48	3.01 ± 0.30

Errors (±) represent standard deviation of mean values of experiments with biological replicates. Min: mineralized/mineralizing; G, G1, G2, and E: extraction steps as defined in the text and in Fig. 1.

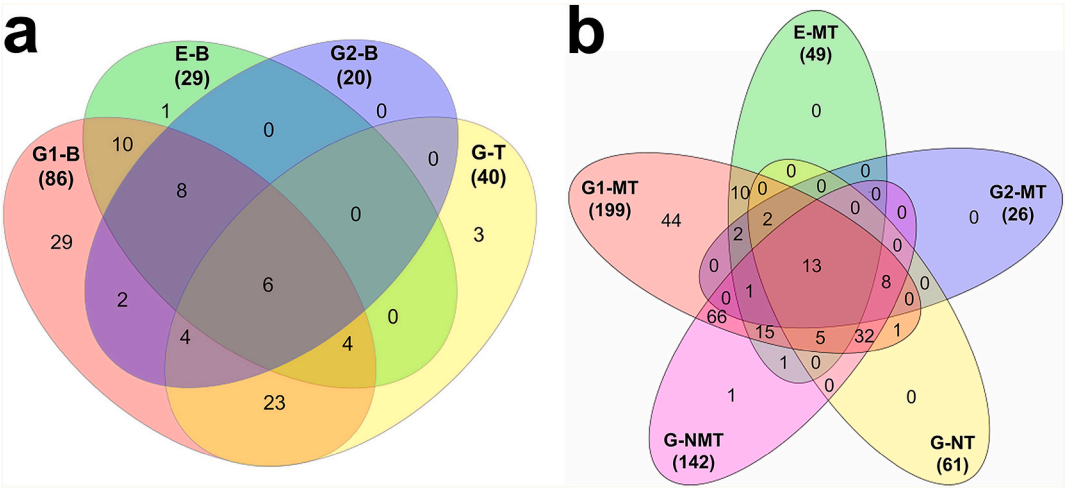

Fig. 2. Venn diagrams of the differential distribution of proteins identified in rat (a) and turkey (b) mineralizing and non-mineralizing tissues. Numbers in parentheses indicate the total proteins that were identified in each extract. Numbers in overlapping regions of the Venn diagrams show the similar proteins that were identified in more than one extract. B: rat bone; T: rat tail tendon; MT: mineralizing TLT; NT: not-yet-mineralized TLT; NMT: never-mineralizing TLT; G, G1, G2, and E: extraction steps as defined in the text and in Fig. 1.

calcification in this tissue by occupying the holes in the gap region of collagen (Scott et al., 1981; Scott and Orford, 1981), where initial nucleation events are principally thought to occur (Landis and Jacquet, 2013). In bone, calcification was reported after the removal of DCN, a result also implying an inhibitory function of DCN in mineral formation (Hoshi et al., 1999). In the current work, DCN was found in high abundance in G2-extracts of rat and turkey mineralizing tissues, a result demonstrating that DCN remains in close association with the collagenous matrix of these mineralizing animal models. In this instance, then, the presence of DCN and other SLRPs in the collagenous matrix (G2) of such mineralizing tissues notably suggests that the long-held hypothesis that these NCPs inhibit mineralization *in vivo* might require reconsideration. Indeed, the association of such NCPs with type I collagen, regardless of the location of the binding sites, may reflect the involvement of these NCPs in only the structural formation or organization of the collagenous matrix rather than in modulating mineralization.

Another group of NCPs that has been associated with bone biomineralization is the SIBLING family. These NCPs are generally highly negatively charged with intrinsically disordered structures and are often post-translationally modified by phosphorylation, which increases NCP acidity. Five NCPs belong to the SIBLING family: osteopontin (OPN), bone sialoprotein (BSP), matrix extracellular phosphoglycoprotein (MEPE), dentin matrix protein 1 (DMP1), and dentin sialophosphoprotein (DSPP) (George and Veis, 2008; Fisher and Fedarko, 2009). With regard to biomineralization, OPN and MEPE have been hypothesized to inhibit mineralization, while BSP, DMP1, and DSPP are suggested to promote bone and dentin mineralization (George and Veis, 2008). These NCPs are expected to be associated with the inorganic components of mineralized tissues. The results of the present proteomics analysis of SIBLING family proteins in rat and turkey tissues are depicted in Fig. 4: Three SIBLING proteins (BSP, DMP1, OPN) were identified in both rat and turkey, while MEPE was identified only in rat (Fig. 4a and b). DSPP was not detected. Interestingly, based on the current proteomics analyses, most of the SIBLINGs were not localized in the non-mineralizing tissues of either rat or turkey. An exception to this result was OPN, which was detected in G-NMT of TLT (never-mineralizing aspect) by proteomics, although even there OPN had conspicuously low abundance and was not detected by Western blotting (Fig. 4d). More importantly and in contrast to the localization of SLRPs, the SIBLINGs were present in highest abundance in the mineral phase of rat and turkey tissues (Fig. 4a and b), an observation which suggests their importance in mineralization.

The relative abundance of OPN in rat and turkey tissues is shown in Fig. 4a and b, respectively. OPN was notably more abundant in the mineral phase of rat bone and the mineralizing portion of TLT compared to the other tissues analyzed. These results were validated by Western blotting in which OPN expression was most prominently shown in E-extracts, indicated by strong bands at ~75 and ~50 kDa for rat and turkey samples, respectively (Fig. 4c and d). Mammalian and avian OPN contains a similar number of amino acids and the nascent protein has a molecular weight of ~34 kDa. OPN is extensively modified by post-translational events, resulting in sizes ranging from 44 to 75 kDa (Prince et al., 1987; Butler, 1989; Sodek et al., 2000; George and Veis, 2008). The molecular weight differences observed in the Western blots are likely reflecting differences in post-translational modifications across the two species (Sodek et al., 2000). Since its original biochemical identification in human, rat and mouse bone, OPN has been consistently localized in the ECM of bone by light microscopy, immunostaining, and Western blotting (Franzen and Heinegard, 1985; Fisher et al., 1987; Prince et al., 1987; Butler, 1989; McKee and Nanci, 1993, 1996; Huang et al., 2008). The current study, however, presents a more specific and detailed spatial distribution of OPN in the inorganic mineral phase of the mineralizing tissues of rat bone and the mineralizing regions of TLT.

Previous investigations have suggested that OPN is a matrix protein not specific to calcified tissues (Butler, 1989) and may function as an inhibitor of dystrophic calcification (Giachelli, 1999; Khan et al., 2002; Giachelli, 2005; Robbiani et al., 2007; Schlieper et al., 2007; Sfiridaki et al., 2011). Despite those studies suggesting that OPN may be found in soft tissues (Khan et al., 2002; Mori et al., 2007; Chen, 2014), the proteomics and Western blotting results in the current work did not reveal the presence of OPN in rat and turkey non-mineralizing tendons, except for the low abundance of OPN only in turkey never-mineralizing tendons. OPN was most abundantly found in the mineral phase of the mineralizing bone and TLT. These results are not consistent with previous observations that OPN is associated with soft tissues; therefore, OPN is hypothesized here to be secreted as an inhibitor of mineralization in soft tissues to mediate and prevent their potential abnormal calcification. The presence of OPN in normally calcifying tissue, especially strictly in the inorganic phase, possibly suggests its proposed role as an inhibitor of crystal growth, thus, preventing excessive mineralization (Jahnen-Dechent et al., 2008; Yuan et al., 2014; Foster et al., 2018).

Fig. 4a and b show the distribution of BSP in rat and turkey tissues, respectively. Similar to OPN, BSP was localized primarily in the E-extracts of both rat and turkey mineralizing tissues. However, BSP was also

Table 2
Relative abundance of ECM proteins across extracts derived from rat mineralizing and non-mineralizing tissues.

Gene name	Description	Bone (B)						Tendon (T)	
		G1		E		G2		G	
		1	2	1	2	1	2	1	2
AHSG	Alpha-2-HS-glycoprotein								
ASPN	Asporin								
BGN	Biglycan								
COL11A1	Collagen alpha-1(XI) chain								
COL12A1	Collagen alpha-1(XII) chain								
COL1A1	Collagen alpha-1(I) chain								
COL2A1	Collagen alpha-1(II) chain								
COL3A1	Collagen alpha-1(III) chain								
COL6A1	Collagen type VI alpha 1 chain								
COL6A2	Collagen type VI alpha 2 chain								
CTSG	Cathepsin G								
DCN	Decorin								
EEF2	Elongation factor 2								
F2	Prothrombin								
FMOD	Fibromodulin								
HIST1H4B	Histone H4								
HSPB1	Heat shock protein beta-1								
LMNA	Prelamin-A/C								
MGP	Matrix Gla protein								
OGN	Osteoglycin								
P4HB	Protein disulfide-isomerase								
RPS11	40S ribosomal protein S11								
SERPINF1	Alpha-2 antiplasmin								
SOST	Sclerostin								
THBS1	Thrombospondin 1								
TUBB5	Tubulin beta-5 chain								
VIM	Vimentin								
VTN	Vitronectin								

min. max.

G, G1, G2, and E: extraction steps as defined in the text and in Fig. 1. 1, 2: Specimens 1 and 2.

detected in G2-extracts of rat bone and mineralizing TLT. These results are in agreement with the presence of ~75 kDa bands detected in both rat and turkey extracts by Western blotting (Fig. 4e and f). BSP concentration in rat was relatively higher in the E-extract than the G2-extract (Fig. 4e), while BSP concentration in turkey was relatively similar in the E- and G2-extracts (Fig. 4f). These results were comparable to the data determined by the present proteomics analyses. BSP is a SIBLING protein that also undergoes extensive post-translational modifications including glycosylation, phosphorylation, and sulfation (Ganss et al., 1999; George and Veis, 2008). These changes can account for up to 50% of the total mass of BSP, which is in the range of 52–82 kDa (George and Veis, 2008). The association of BSP with the organic phase

Table 3
Relative abundance of ECM proteins across extracts derived from turkey mineralizing and non-mineralizing tissues.

Gene name	Description RefSeq	Turkey leg tendon									
		Mineralizing (MT)						Not-yet-min (NT)		Never-min (NMT)	
		G1		E		G2		G		G	
		1	2	1	2	1	2	1	2	1	2
CILP	Cartilage intermediate layer protein 1										
CLU	Clusterin										
COMP	Cartilage oligomeric matrix protein										
DCN	Decorin										
HNRNPM	Heterogeneous nuclear ribonucleoprotein M										
HSPG2	Heparan sulfate proteoglycan core protein										
LMCD1	LIM & cysteine-rich domains protein 1										
MFGE8	Lactadherin isoform X2										
MGP	Matrix Gla protein										
OGN	Mimecan										
OMD	Osteomodulin										
PKM	Pyruvate kinase PKM isoform X2										
SERPINF1	Pigment epithelium-derived factor										
SOST	Sclerostin isoform X2										
THBS1	Thrombospondin 1										
TNC	Tenascin isoform X9										
COL6A2	Collagen alpha-2(VI) chain isoform X1										
COL1A2	Collagen alpha-2(I) chain										
COL6A1	Collagen alpha-1(VI) chain										
COL5A2	Collagen alpha-2(V) chain isoform X2										
COL1A1	Collagen alpha-1(I) chain-like partial										
COL12A1	Collagen alpha-1(XII) chain										
COL16A1	Collagen alpha-1(XVI) chain										

*: inserted manually to include collagen chain proteins. Min: mineralized/mineralizing; G, G1, G2, and E: extraction steps as defined in the text and in Fig. 1. 1, 2: Specimens 1 and 2.

of mineralized tissues found here is consistent with results from previous investigations (Chen et al., 1994; Laboux et al., 2003; Chen et al., 2015).

BSP has been thought to have a high affinity for HAP, a conclusion leading to suggestions of its role in promoting biomineralization (George and Veis, 2008). Studies *in vitro* report that BSP may function as a nucleator of HAP because of its consistent presence in mineralizing tissues such as bone, dentin, and calcifying cartilage (George and Veis, 2008), and because BSP function in such a capacity was primarily related to its post-translational modifications (Hunter and Goldberg, 1993; Hunter et al., 1996; Stubbs et al., 1997; Zhu et al., 2001; Baht et al., 2008; George and Veis, 2008). Immunogold localization studies have previously revealed that BSP was associated with electron-dense material in the mineralized matrices of porcine calvarial bone, rat tibiae, and TLT (Chen et al., 1994; Laboux et al., 2003; Chen et al., 2015). Knockout studies of BSP in mice showed that the animals were viable and not devoid of bone formation, though they exhibited altered bone properties (Malaval et al., 2008). In the current work, BSP was found in low abundance in the G2-extracts, data indicating its association with the organic collagenous matrix after the mineral phase was removed. This result suggests that BSP might be an initiator of intrafibrillar collagen mineralization. BSP was found in highest abundance in the inorganic mineral phase of the tissues investigated, a result suggesting that it might be secreted in later stages of mineralization, so as to regulate events of crystal growth or extrafibrillar collagen mineralization.

Another family of NCPs that has been widely associated with

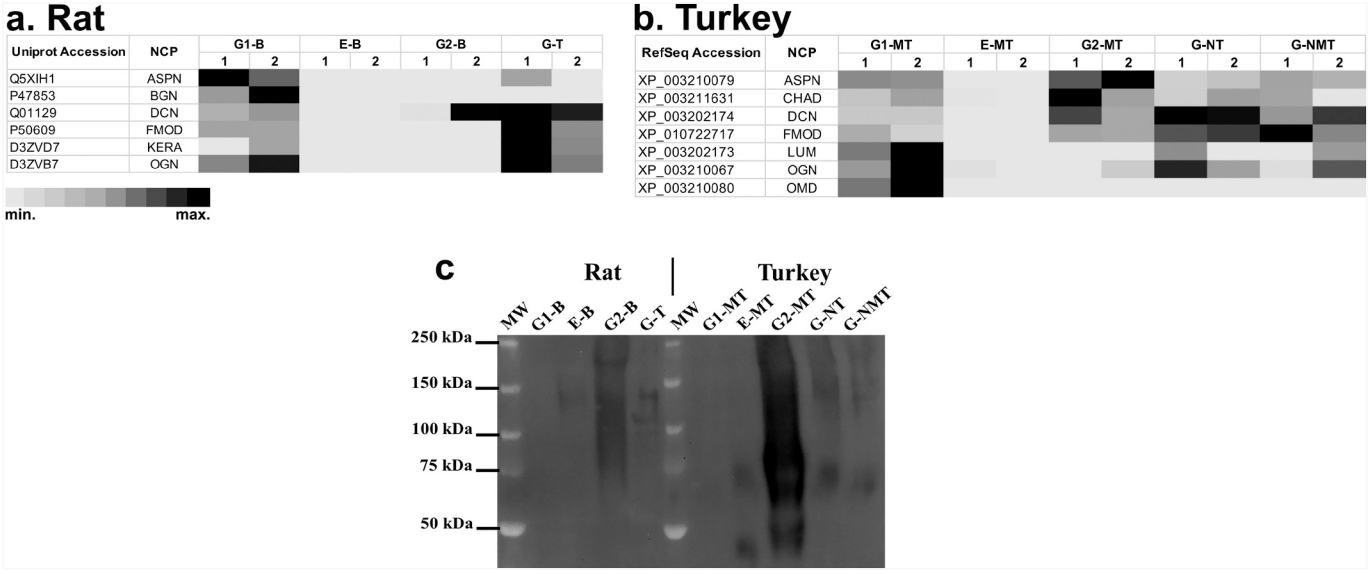

Fig. 3. The relative distribution of SLRP proteins in extracts derived from rat (a) and turkey (b) mineralizing and non-mineralizing tissues. Validation of decorin (DCN) localization by Western blotting (c). B: rat bone; T: rat tail tendon; MT: mineralizing TLT; NT: not-yet-mineralized TLT; NMT: never-mineralizing TLT. G, G1, G2, and E: extraction steps as defined in the text and in Fig. 1. 1, 2: Specimens 1 and 2.

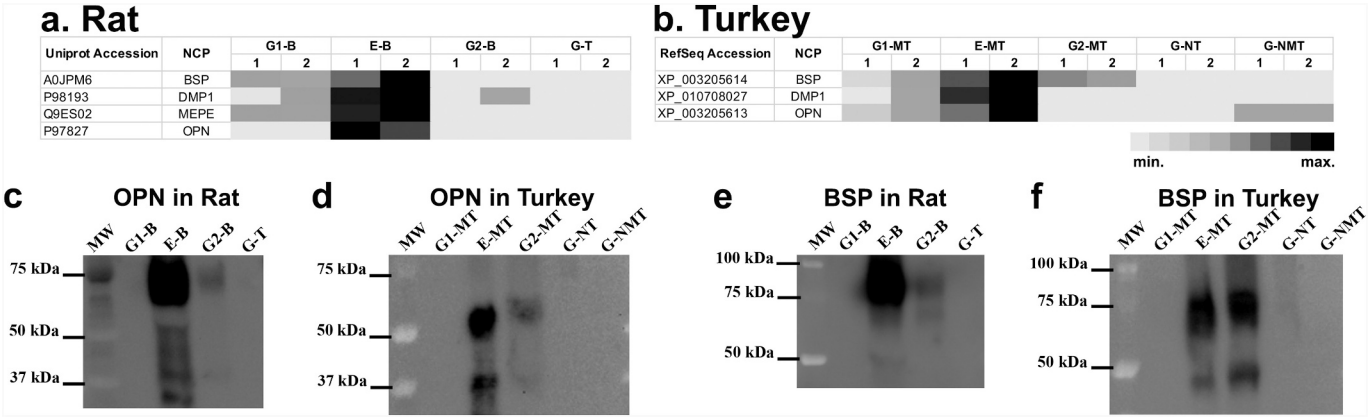

Fig. 4. The relative distribution of SIBLING proteins in extracts derived from rat (a) and turkey (b) mineralizing and non-mineralizing tissues and Western blot-based validation of the localization of OPN in rat (c) and turkey (d) and BSP in rat (e) and turkey (f) tissues. B: rat bone; T: rat tail tendon; MT: mineralizing TLT; NT: not-yet-mineralized TLT; NMT: never-mineralizing TLT. G, G1, G2, and E: extraction steps as defined in the text and in Fig. 1. 1, 2: Specimens 1 and 2.

mineralization is that of the mineral-binding γ-carboxylated glutamic acid (Gla) proteins, which include, among others, matrix Gla protein (MGP) and osteocalcin/bone Gla protein (OCN). These NCPs belong to a group of vitamin K-dependent proteins, in which γ-carboxylation of their Glu residues depends on the presence of vitamin K as a cofactor. The Gla residues endow these proteins with a high affinity for calcium ions and HAP crystals. Matrix Gla protein is a ~14-kDa NCP with reported four and five Gla residues in murine and bovine species, respectively (Price et al., 1983; Price and Williamson, 1985; Hauschka et al., 1989). Despite being initially isolated from bone (Price and Williamson, 1985), MGP has been suggested as an active inhibitor of calcification in soft tissues such as cartilage and arteries. An MGP-knockout study in mice reported severe calcification of the vasculature of the animals and showed accelerated and premature mineralization of their normally mineralizing cartilage and bone growth plate relative to the control (Luo et al., 1997). Previously, MGP was thought to be associated with both the mineral and collagenous matrix of developing bone (Hauschka et al., 1989). The current proteomics study, however, revealed that MGP was most abundant in the mineral phase of rat bone, as expected, and of mineralizing TLT as well (Fig. 5a and b). This result correlates with the localization found here for the SIBLING family of proteins, which is considered to play an important role in mineralization.

OCN was detected in only the mineralizing tissues of rat and turkey by proteomics analysis. In rat, OCN was found with the highest abundance in the G1-extract (Fig. 5a), but it was most concentrated in E-extracts in turkey (Fig. 5b). In both species, however, OCN was found associated with cellular, collagenous, and mineral phases of the tissues. Western blot results localized OCN bands at ~10 kDa in only E-extracts in both rat and turkey mineralizing tissues (Fig. 5c). The inconsistency observed between OCN proteomics and Western blot results might be the consequence of the difference in post-translational modifications. The Western blot localization of OCN in only mineralizing tissues, however, is consistent with earlier studies that have documented the localization of OCN in mineralized bone matrix of monkey vertebrae, rat femurs and tibiae, rat teeth, and chicken tibiae (Bronckers et al., 1985; Bronckers et al., 1987; McKee et al., 1992; Carlson et al., 1993). OCN was previously reported to be absent in osteoid or predentin, both of which lack mineral (Bronckers et al., 1985; Bronckers et al., 1987; McKee et al., 1992; Carlson et al., 1993). In addition, the presence of

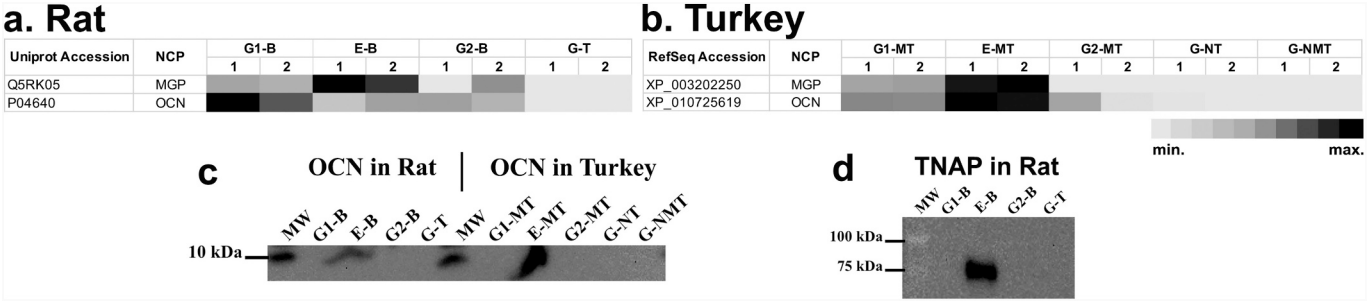

Fig. 5. The identification of vitamin K-dependent NCPs in rat and turkey and a comparison of MGP abundance in rat (a) and turkey (b). The identification of OCN in rat and turkey is validated by Western blotting (c). Western blot results of tissue-nonspecific alkaline phosphatase (TNAP) in rat bone and tail tendon (d). B: rat bone; T: rat tail tendon; MT: mineralizing TLT; NT: not-yet-mineralized TLT; NMT: never-mineralizing TLT. G, G1, G2, and E: extraction steps as defined in the text and in Fig. 1. 1, 2: Specimens 1 and 2.

OCN in the mineralizing tissues, especially in bone, should not come as a surprise as Ducy et al. found that, in the absence of this protein, the phenotype of bone was altered (Ducy et al., 1996).

OCN has long been proposed to play an active role in mineralization because of its being osteoblast-specific (Hauschka et al., 1989; Oldknow et al., 2015). However, it recently was also found to be expressed by tenocytes in mineralizing turkey tendons (Chen et al., 2015). In agreement with Chen et al. (2015), our study found OCN in mineralizing turkey tendon by both proteomics and Western blotting. Interestingly, the proteomics results in the present study (Supplemental Fig. 1) showed that the Glu residues of OCN in turkey were not γ-carboxylated, but instead the data identified β-carboxylated Asp residues (Asa). Asa post-translational modification has been previously identified in *E. coli* ribosomal proteins (Christy et al., 1981). Similar to Gla, the carboxylation of Asp is mediated by vitamin K, and Asa has been detected among other vitamin K-dependent proteins such as factor IX, factor X, and protein C (Drakenberg et al., 1983; Fernlund and Stenflo, 1983). The finding of β-carboxylation of Asp in OCN may be important in relation to the hypothesized role of OCN in mineralization, as discussed below.

Previous studies *in vitro* have suggested that OCN regulates the maturation of bone minerals by inhibiting mineral formation or delaying apatite nucleation (Boskey et al., 1985; Hunter et al., 1996; Flade et al., 2001). The crystal structure of OCN shows that its γ-carboxylate residues are spaced at a distance that is complementary to calcium ions comprising the (100) face of HAP and, hence, it was considered to template HAP crystal growth (Hoang et al., 2003). OCN associates with calcium ions though its Gla residues and molecular dynamics simulations of OCN interactions with Ca^{2+} and $(HPO_4)^{2-}$ ions in solution show that OCN promotes calcium phosphate cluster formation (Hauschka and Wians Jr., 1989; Hauschka et al., 1989; Zhao et al., 2018; Wang et al., 2020). OCN has also been recognized as a prohormone for its future release during osteoclastic bone resorption (Ducy, 2011; Wei and Karsenty, 2015; Zoch et al., 2016). However, recent studies raise questions about endocrinal or hormonal function of OCN (Diegel et al., 2020; Moriishi et al., 2020). Morrishi et al. instead found that the presence of OCN is vital in aligning the HAP crystals along the *c*-axis of type I collagen fibrils (Moriishi et al., 2020).

Together with previous findings *in vivo* (Ducy et al., 1996; Luo et al., 1997; Murshed et al., 2004; Kaipatur et al., 2008), our proteomics results indicate that MGP, which also has Gla residues as noted above, is associated with the mineral phase of both rat bone and mineralizing regions of turkey tendon (Fig. 5a and b). In summary, OCN appears in various extracts of mineralizing tissues, whereas MGP is associated only with the mineral phase of mineralizing tissues, similar to the results previously noted for the SIBLINGs. Such an association suggests that both MGP and OCN might play a role in bone mineralization, where the role of MGP is possibly related to inhibition (Luo et al., 1997; Schinke et al., 1999; Murshed et al., 2004; Dan et al., 2012). Our findings on OCN do not preclude its role as a hormone.

Another protein that has been proposed to play an important role in mineralization is tissue-nonspecific alkaline phosphatase (TNAP). TNAP has been detected in ECM vesicles in bone, cartilage and other mineralizing tissues and is the principal regulating enzyme of inorganic pyrophosphate (Addison et al., 2007). Inorganic pyrophosphate is an inhibitor of soft tissue mineralization (Addison et al., 2007). The critical importance of TNAP in proper skeletal mineralization has been extensively studied and reviewed in the literature (Wennberg et al., 2000; Hessle et al., 2002; Murshed and McKee, 2010; Millán, 2013; Huesa et al., 2015). Studies have shown that TNAP deficiency is associated with hypophosphatasia affecting a range of mineralizing tissues, such as craniofacial and long bones as well as teeth (Liu et al., 2014; Millan and Whyte, 2016). The presence of TNAP in mineralizing tissues such as bone, including rat tibia and femur, and teeth has previously been reported (Hotton et al., 1999; Miao and Scutt, 2002; Hosoya et al., 2006). In soft tissues, TNAP was found abundantly in liver and kidney, as well as in rat cartilage and growth plate (Hosoya et al., 2006; McKenna et al., 1979). A different perspective of the role of TNAP has been offered by the work of Murshed and coworkers (Murshed et al., 2004, 2005). They have proposed that the only requirement for vertebrate mineralization is the co-localization of TNAP with collagen (Murshed et al., 2004; Murshed et al., 2005; Murshed and McKee, 2010). In our study TNAP was not detected in rat tail tendon, but only in the E-extract of rat bone by Western blotting (Fig. 5d). The lack of a turkey-specific antibody for TNAP prevented its identification in TLTs by Western blotting. The current study does not directly address possible roles of TNAP in mineralization, but the localization of TNAP to only the mineral phase, similar to that of both SIBLING proteins and MGP, is intriguing. Our findings may support the concept that TNAP is actively involved in initiating mineralization, as proposed by several others (Murshed et al., 2004; Murshed et al., 2005; Ducy, 2011; Wei and Karsenty, 2015; Zoch et al., 2016).

4. Conclusions

This study reports the results of unique and carefully designed approaches to examine NCPs in vertebrate mineralizing tissues from male species. These methodologies include: (1) an investigation of two different animal models, rat and turkey, studied *ex vivo* to quantify NCPs in their mineralizing and non-mineralizing tissues and to determine whether certain NCPs are specific to each tissue type; and (2) a novel combination of sequential protein extractions followed by proteomics and Western blot analyses. NCPs were strictly extracted based on their association with different phases of the ECM, that is, the organic collagenous and inorganic mineral phases, or both, of the tissues examined. This protocol allowed a number of novel findings to come to light. Importantly, the results provided here are not limited to individual NCPs but can be generalized to various protein families and thus are relevant more broadly in this context. In particular, existing literature

has shown that SLRPs are found in mineralized tissues, and hence it has been proposed that they may be either inhibitors of mineralization or regulators of organic collagenous matrix organization or both. Our study has shown, for the first time, that various SLRPs are found strictly associated with the organic collagenous phase alone and not with the inorganic mineral phase of mineralized tissues. This result suggests that the role of SLRPs might be limited only to structural organic matrix organization and not to inhibition of mineralization. In contrast, we additionally found that the SIBLING family, along with MGP, is closely associated with the mineral phase of mineralized tissues, a result confirming previous suggestions that the SIBLINGS play important roles in mineralization. We also found that OCN may be involved in regulating mineralization, but the findings here did not preclude its potential role as a systemic hormone. Moreover, with the caveat of experimental limitations of the current study, the localization of TNAP was confined to the inorganic mineral phase of rat femur, a result which is consistent with its proposed role in promoting mineralization. Based on our data, we believe that our study helps clarify the hypothesized functions of these important proteins/protein families in biomineralization. Further studies using additional animal models, including specific genetic modifications, combined with proteomics and Western blot analyses, should expand understanding of the roles of additional proteins in vertebrate mineralization.

Supplementary data to this article can be found online at https://doi.org/10.1016/j.bonr.2021.100754.

CRediT authorship contribution statement

Putu Ustriyana: Conceptualization, Methodology, Investigation, Software, Validation, Formal analysis, Writing – original draft, Visualization. **Fabian Schulte:** Methodology, Investigation, Formal analysis, Software, Writing – review & editing. **Farai Gombedza:** Methodology, Validation, Investigation, Formal analysis, Writing – review & editing. **Ana Gil-Bona:** Methodology, Investigation, Writing – review & editing. **Sailaja Paruchuri:** Writing – review & editing, Supervision. **Felicitas B. Bidlack:** Writing – review & editing, Supervision. **Markus Hardt:** Software, Formal analysis, Writing – review & editing, Supervision. **William J. Landis:** Conceptualization, Writing – review & editing, Supervision. **Nita Sahai:** Conceptualization, Writing – review & editing, Supervision, Funding acquisition.

Declaration of competing interest

The authors declare that they have no known competing financial interests or personal relationships that could have appeared to influence the work reported in this paper.

Acknowledgements

We are grateful to Dr. Larry W. Fisher (NIDCR/NIH) and Dr. Marc D. McKee (McGill University) for generously providing primary antibodies needed for this project. We acknowledge Dr. Chunlin Qin (Texas A&M University) for kindly sharing his research protocol and experiences; the laboratory group of Dr. Nic Leipzig (The University of Akron) for providing tissues during preliminary studies; and Ms. Robin DiFeo Childs and Dr. Ling Chen (The University of Akron) for valuable suggestions in the optimization of Western blotting methods. We appreciate the great help of Ms. Kelly Stevanov and Dr. Walter Horne (The University of Akron Research Vivarium) with animal protocols. We also thank the Fulbright Foundation and the US Department of State for a scholarship awarded to PU.

Funding: This work was supported by start-up funds from The University of Akron to NS and The Robert Helm, Jr., Fellowship in Polymers and Biomaterials awarded to PU. The Forsyth Center for Salivary Diagnostics was funded by the Massachusetts Life Science Center.

References

Addison, W.N., Azari, F., Sorensen, E.S., Kaartinen, M.T., McKee, M.D., 2007. Pyrophosphate inhibits mineralization of osteoblast cultures by binding to mineral, up-regulating osteopontin, and inhibiting alkaline phosphatase activity. J. Biol. Chem. 282 (21), 15872–15883.

Aslan, H., Kimelman-Bleich, N., Pelled, G., Gazit, D., 2008. Molecular targets for tendon neoformation. J. Clin. Invest. 118 (2), 439–444.

Baht, G.S., Hunter, G.K., Goldberg, H.A., 2008. Bone sialoprotein-collagen interaction promotes hydroxyapatite nucleation. Matrix Biol. 27 (7), 600–608.

Beniash, E., 2011. Biominerals-hierarchical nanocomposites: the example of bone. Wiley Interdisciplinary Reviews-Nanomedicine and Nanobiotechnology 3 (1), 47–69.

Berthet-Colominas, C., Miller, A., White, S.W., 1979. Structural study of the calcifying collagen in turkey leg tendons. J. Mol. Biol. 134 (3), 431–445.

Bianco, P., Fisher, L.W., Young, M.F., Termine, J.D., Robey, P.G., 1990. Expression and localization of the two small proteoglycans biglycan and decorin in developing human skeletal and non-skeletal tissues. J. Histochem. Cytochem. 38 (11), 1549–1563.

Boskey, A.L., 1989. Noncollagenous matrix proteins and their role in mineralization. Bone and Mineral 6 (2), 111–123.

Boskey, A.L., Wians Jr., F.H., Hauschka, P.V., 1985. The effect of osteocalcin onIn vitro lipid-induced hydroxyapatite formation and seeded hydroxyapatite growth. Calcif. Tissue Int. 37 (1), 57–62.

Boskey, A.L., Gadaleta, S., Gundberg, C., Doty, S.B., Ducy, P., Karsenty, G., 1998. Fourier transform infrared microspectroscopic analysis of bones of osteocalcin-deficient mice provides insight into the function of osteocalcin. Bone 23 (3), 187–196.

Bronckers, A.L., Gay, S., Dimuzio, M.T., Butler, W.T., 1985. Immunolocalization of gamma-carboxyglutamic acid containing proteins in developing rat bones. Coll. Relat. Res. 5 (3), 273–281.

Bronckers, A.L.J.J., Gay, S., Finkelman, R.D., Butler, W.T., 1987. Immunolocalization of Gla proteins (osteocalcin) in rat tooth germs - comparison between indirect immunofluorescence, peroxidase-antiperoxidase, avidin-biotin-peroxidase complex, and avidin-biotin-gold complex with silver enhancement. J. Histochem. Cytochem. 35 (8), 825–830.

Butler, W.T., 1989. The nature and significance of osteopontin. Connect. Tissue Res. 23 (2–3), 123–136.

Carlson, C.S., Tulli, H.M., Jayo, M.J., Loeser, R.F., Tracy, R.P., Mann, K.G., Adams, M.R., 1993. Immunolocalization of noncollagenous bone matrix proteins in lumbar vertebrae from intact and surgically menopausal cynomolgus monkeys. J. Bone Miner. Res. 8 (1), 71–81.

Chen, L., 2014. Characterization of Non-collagenous Proteins in Vertebrate Mineralization. The University of Akron.

Chen, S., Birk, D.E., 2013. The regulatory roles of small leucine-rich proteoglycans in extracellular matrix assembly. FEBS J. 280 (10), 2120–2137.

Chen, J., McKee, M.D., Nanci, A., Sodek, J., 1994. Bone sialoprotein mRNA expression and ultrastructural localization in fetal porcine calvarial bone: comparisons with osteopontin. Histochem. J. 26 (1), 67–78.

Chen, L., Jacquet, R., Lowder, E., Landis, W.J., 2015. Refinement of collagen-mineral interaction: a possible role for osteocalcin in apatite crystal nucleation, growth and development. Bone 71, 7–16.

M.R. Christy, R.M. Barkley, T.H. Koch, J.J. Van Buskirk, W.M. Kirsch, The new amino acid .beta.-carboxyaspartic acid (asa). Laboratory synthesis and identification in the ribosomal proteins of *E. coli*, Journal of the American Chemical Society 103(13) (1981) 3935–3937.

Dan, H., Simsa-Maziel, S., Reich, A., Sela-Donenfeld, D., Monsonego-Ornan, E., 2012. The role of matrix gla protein in ossification and recovery of the avian growth plate. Front Endocrinol (Lausanne) 3, 79.

Danielson, K.G., Baribault, H., Holmes, D.F., Graham, H., Kadler, K.E., Iozzo, R.V., 1997. Targeted disruption of decorin leads to abnormal collagen fibril morphology and skin fragility. J. Cell Biol. 136 (3), 729–743.

Diegel, C.R., Hann, S., Ayturk, U.M., Hu, J.C.W., Lim, K.E., Droscha, C.J., Madaj, Z.B., Foxa, G.E., Izaguirre, I., Transgenics Core, V.V.A., Paracha, N., Pidhaynyy, B., Dowd, T.L., Robling, A.G., Warman, M.L., Williams, B.O., 2020. An osteocalcin-deficient mouse strain without endocrine abnormalities. PLoS Genet. 16 (5), e1008361.

Domenicucci, C., Goldberg, H.A., Hofmann, T., Isenman, D., Wasi, S., Sodek, J., 1988. Characterization of porcine osteonectin extracted from foetal calvariae. Biochem. J. 253 (1), 139–151.

T. Drakenberg, P. Fernlund, P. Roepstorff, J. Stenflo, beta-Hydroxyaspartic acid in vitamin K-dependent protein C, Proc Natl Acad Sci U S A 80 (7) (1983) 1802–6.

Duah, E., Adapala, R.K., Al-Azzam, N., Kondeti, V., Gombedza, F., Thodeti, C.K., Paruchuri, S., 2013. Cysteinyl leukotrienes regulate endothelial cell inflammatory and proliferative signals through CysLT(2) and CysLT(1) receptors. Sci. Rep. 3, 3274.

Ducy, P., 2011. The role of osteocalcin in the endocrine cross-talk between bone remodelling and energy metabolism. Diabetologia 54 (6), 1291–1297.

Ducy, P., Desbois, C., Boyce, B., Pinero, G., Story, B., Dunstan, C., Smith, E., Bonadio, J., Goldstein, S., Gundberg, C., Bradley, A., Karsenty, G., 1996. Increased bone formation in osteocalcin-deficient mice. Nature 382 (6590), 448–452.

Fernlund, P., Stenflo, J., 1983. Beta-hydroxyaspartic acid in vitamin K-dependent proteins. J. Biol. Chem. 258 (20), 12509–12512.

Fisher, L.W., Fedarko, N.S., 2009. Six genes expressed in bones and teeth encode the current members of the SIBLING family of proteins. Connect. Tissue Res. 44 (1), 33–40.

Fisher, L.W., Termine, J.D., Dejter Jr., S.W., Whitson, S.W., Yanagishita, M., Kimura, J. H., Hascall, V.C., Kleinman, H.K., Hassell, J.R., Nilsson, B., 1983. Proteoglycans of developing bone. J. Biol. Chem. 258 (10), 6588–6594.

Fisher, L.W., Hawkins, G.R., Tuross, N., Termine, J.D., 1987. Purification and partial characterization of small proteoglycans I and II, bone sialoproteins I and II, and osteonectin from the mineral compartment of developing human bone. J. Biol. Chem. 262 (20), 9702–9708.
Flade, K., Lau, C., Mertig, M., Pompe, W., 2001. Osteocalcin-controlled dissolution-reprecipitation of calcium phosphate under biomimetic conditions. Chem. Mater. 13 (10), 3596–3602.
Foster, B.L., Ao, M., Salmon, C.R., Chavez, M.B., Kolli, T.N., Tran, A.B., Chu, E.Y., Kantovitz, K.R., Yadav, M., Narisawa, S., Millan, J.L., Nociti Jr., F.H., Somerman, M. J., 2018. Osteopontin regulates dentin and alveolar bone development and mineralization. Bone 107, 196–207.
Franzen, A., Heinegard, D., 1985. Isolation and characterization of two sialoproteins present only in bone calcified matrix. Biochem. J. 232 (3), 715–724.
Ganss, B., Kim, R.H., Sodek, J., 1999. Bone sialoprotein. Crit. Rev. Oral Biol. Med. 10 (1), 79–98.
George, A., Veis, A., 2008. Phosphorylated proteins and control over apatite nucleation, crystal growth, and inhibition. Chem. Rev. 108 (11), 4670–4693.
Giachelli, C.M., 1999. Ectopic calcification: gathering hard facts about soft tissue mineralization. Am. J. Pathol. 154 (3), 671–675.
Giachelli, C.M., 2005. Inducers and inhibitors of biomineralization: lessons from pathological calcification. Orthod Craniofac Res 8 (4), 229–231.
Glimcher, M.J., 2006. Bone: nature of the calcium phosphate crystals and cellular, structural, and physical chemical mechanisms in their formation. Medical Mineraology and Geochemistry 64 (1), 223–282.
Glimcher, M.J., Hodge, A.J., Schmitt, F.O., 1957. Macromolecular aggregation states in relation to mineralization: the collagen-hydroxyapatite system as studied in vitro. Proc. Natl. Acad. Sci. U. S. A. 43 (10), 860–867.
Gorski, J.P., 1992. Acidic phosphoproteins from bone matrix: a structural rationalization of their role in biomineralization. Calcif. Tissue Int. 50 (5), 391–396.
Hauschka, P.V., Wians Jr., F.H., 1989. Osteocalcin-hydroxyapatite interaction in the extracellular organic matrix of bone. Anat. Rec. 224 (2), 180–188.
Hauschka, P.V., Lian, J.B., Cole, D.E., Gundberg, C.M., 1989. Osteocalcin and matrix Gla protein: vitamin K-dependent proteins in bone. Physiol. Rev. 69 (3), 990–1047.
Hessle, L., Johnson, K.A., Anderson, H.C., Narisawa, S., Sali, A., Goding, J.W., Terkeltaub, R., Millán, J.L., 2002. Tissue-nonspecific alkaline phosphatase and plasma cell membrane glycoprotein-1 are central antagonistic regulators of bone mineralization. Proc. Natl. Acad. Sci. U. S. A. 99 (14), 9445–9449.
Hoang, Q.Q., Sicheri, F., Howard, A.J., Yang, D.S., 2003. Bone recognition mechanism of porcine osteocalcin from crystal structure. Nature 425 (6961), 977–980.
Holm, E., Aubin, J.E., Hunter, G.K., Beier, F., Goldberg, H.A., 2015. Loss of bone sialoprotein leads to impaired endochondral bone development and mineralization. Bone 71, 145–154.
Hoshi, K., Kemmotsu, S., Takeuchi, Y., Amizuka, N., Ozawa, H., 1999. The primary calcification in bones follows removal of decorin and fusion of collagen fibrils. J. Bone Miner. Res. 14 (2), 273–280.
Hosoya, A., Nakamura, H., Ninomiya, T., Yoshiba, K., Yoshiba, N., Nakaya, H., Wakitani, S., Yamada, H., Kasahara, E., Ozawa, H., 2006. Immunohistochemical localization of alpha-smooth muscle actin during rat molar tooth development. J. Histochem. Cytochem. 54 (12), 1371–1378.
Hotton, D., Mauro, N., Lezot, F., Forest, N., Berdal, A., 1999. Differential expression and activity of tissue-nonspecific alkaline phosphatase (TNAP) in rat odontogenic cells in vivo. J. Histochem. Cytochem. 47 (12), 1541–1552.
Huang, B., Sun, Y., Maciejewska, I., Qin, D., Peng, T., McIntyre, B., Wygant, J., Butler, W. T., Qin, C., 2008. Distribution of SIBLING proteins in the organic and inorganic phases of rat dentin and bone. Eur. J. Oral Sci. 116 (2), 104–112.
Huesa, C., Houston, D., Kiffer-Moreira, T., Yadav, M.M., Millan, J.L., Farquharson, C., 2015. The functional co-operativity of tissue-nonspecific alkaline phosphatase (TNAP) and PHOSPHO1 during initiation of skeletal mineralization. Biochem Biophys Rep 4, 196–201.
Hunter, G.K., Goldberg, H.A., 1993. Nucleation of hydroxyapatite by bone sialoprotein. Proc. Natl. Acad. Sci. U. S. A. 90 (18), 8562–8565.
G.K. Hunter, P.V. Hauschka, A.R. Poole, L.C. Rosenberg, H.A. Goldberg, Nucleation and inhibition of hydroxyapatite formation by mineralized tissue proteins, Biochem J 317 (Pt 1) (1) (1996) 59–64.
Jahnen-Dechent, W., Schafer, C., Ketteler, M., McKee, M.D., 2008. Mineral chaperones: a role for fetuin-A and osteopontin in the inhibition and regression of pathologic calcification. J Mol Med (Berl) 86 (4), 379–389.
Kaipatur, N.R., Murshed, M., McKee, M.D., 2008. Matrix Gla protein inhibition of tooth mineralization. J. Dent. Res. 87 (9), 839–844.
Kannus, P., 2000. Structure of the tendon connective tissue. Scand. J. Med. Sci. Sports 10 (6), 312–320.
Khan, S.R., Johnson, J.M., Peck, A.B., Cornelius, J.G., Glenton, P.A., 2002. Expression of osteopontin in rat kidneys: induction during ethylene glycol induced calcium oxalate nephrolithiasis. J. Urol. 168 (3), 1173–1181.
Kuwabara, M., Takuma, T., Scott, P.G., Dodd, C.M., Mizoguchi, I., 2002. Biochemical and immunohistochemical studies of the protein expression and localization of decorin and biglycan in the temporomandibular joint disc of growing rats. Arch. Oral Biol. 47 (6), 473–480.
Laboux, O., Ste-Marie, L., Glorieux, F., Nanci, A., 2003. Quantitative immunogold labeling of bone sialoprotein and osteopontin in methylmethacrylate-embedded rat bone. J. Histochem. Cytochem. 51 (1), 61–67.
Landis, W.J., 1986. A study of calcification in the leg tendons from the domestic turkey. J. Ultrastruct. Mol. Struct. Res. 94 (3), 217–238.
Landis, W.J., Jacquet, R., 2013. Association of calcium and phosphate ions with collagen in the mineralization of vertebrate tissues. Calcif. Tissue Int. 93 (4), 329–337.
Landis, W.J., Silver, F.H., 2002. The structure and function of normally mineralizing avian tendons. Comp. Biochem. Physiol. A Mol. Integr. Physiol. 133 (4), 1135–1157.
Landis, W.J., Song, M.J., 1991. Early mineral deposition in calcifying tendon characterized by high voltage electron microscopy and three-dimensional graphic imaging. J. Struct. Biol. 107 (2), 116–127.
Landis, W., Song, M., Leith, A., McEwen, L., McEwen, B., 1993. Mineral and organic matrix interaction in normally calcifying tendon visualized in three dimensions by high-voltage electron microscopic tomography and graphic image reconstruction. J. Struct. Biol. 110 (1), 39–54.
Landis, W.J., Hodgens, K.J., Song, M.J., Arena, J., Kiyonaga, S., Marko, M., Owen, C., McEwen, B.F., 1996. Mineralization of collagen may occur on fibril surfaces: evidence from conventional and high-voltage electron microscopy and three-dimensional imaging. J. Struct. Biol. 117 (1), 24–35.
Landis, W.J., Kraus, B.L.H., Kirker-Head, C.A., 2002. Vascular-mineral spatial correlation in the calcifying turkey leg tendon. Connect. Tissue Res. 43 (4), 595–605.
Liu, J., Nam, H.K., Campbell, C., Gasque, K.C., Millan, J.L., Hatch, N.E., 2014. Tissue-nonspecific alkaline phosphatase deficiency causes abnormal craniofacial bone development in the Alpl(−/−) mouse model of infantile hypophosphatasia. Bone 67, 81–94.
Luo, G., Ducy, P., McKee, M.D., Pinero, G.J., Loyer, E., Behringer, R.R., Karsenty, G., 1997. Spontaneous calcification of arteries and cartilage in mice lacking matrix GLA protein. Nature 386 (6620), 78–81.
Malaval, L., Wade-Guéye, N.M., Boudiffa, M., Fei, J., Zirngibl, R., Chen, F., Laroche, N., Roux, J.-P., Burt-Pichat, B., Duboeuf, F., 2008. Bone sialoprotein plays a functional role in bone formation and osteoclastogenesis. J. Exp. Med. 205 (5), 1145–1153.
McKee, M., Nanci, A., 1993. Ultrastructural, cytochemical and immunocytochemical studies on bone and its interfaces. Cells Mater. 3 (3), 219–243.
McKee, M., Nanci, A., 1996. Osteopontin at mineralized tissue interfaces in bone, teeth, and osseointegrated implants: ultrastructural distribution and implications for mineralized tissue formation, turnover, and repair. Microsc. Res. Tech. 33 (2), 141–164.
McKee, M., Glimcher, M., Nanci, A., 1992. High-resolution immunolocalization of osteopontin and osteocalcin in bone and cartilage during endochondral ossification in the chicken tibia. Anat. Rec. 234 (4), 479–492.
McKenna, M.J., Hamilton, T.A., Sussman, H.H., 1979. Comparison of human alkaline phosphatase isoenzymes. Structural evidence for three protein classes, Biochemical Journal 181 (1), 67–73.
Miao, D., Scutt, A., 2002. Histochemical localization of alkaline phosphatase activity in decalcified bone and cartilage. J. Histochem. Cytochem. 50 (3), 333–340.
Millán, J.L., 2013. The role of phosphatases in the initiation of skeletal mineralization. Calcif. Tissue Int. 93 (4), 299–306.
Millan, J.L., Whyte, M.P., 2016. Alkaline phosphatase and hypophosphatasia. Calcif. Tissue Int. 98 (4), 398–416.
Mori, N., Majima, T., Iwasaki, N., Kon, S., Miyakawa, K., Kimura, C., Tanaka, K., Denhardt, D.T., Rittling, S., Minami, A., 2007. The role of osteopontin in tendon tissue remodeling after denervation-induced mechanical stress deprivation. Matrix Biol. 26 (1), 42–53.
Moriishi, T., Ozasa, R., Ishimoto, T., Nakano, T., Hasegawa, T., Miyazaki, T., Liu, W., Fukuyama, R., Wang, Y., Komori, H., Qin, X., Amizuka, N., Komori, T., 2020. Osteocalcin is necessary for the alignment of apatite crystallites, but not glucose metabolism, testosterone synthesis, or muscle mass. PLoS Genet. 16 (5), e1008586.
Murshed, M., McKee, M.D., 2010. Molecular determinants of extracellular matrix mineralization in bone and blood vessels. Curr. Opin. Nephrol. Hypertens. 19 (4), 359–365.
Murshed, M., Schinke, T., McKee, M.D., Karsenty, G., 2004. Extracellular matrix mineralization is regulated locally; different roles of two gla-containing proteins. J. Cell Biol. 165 (5), 625–630.
Murshed, M., Harmey, D., Millán, J.L., McKee, M.D., Karsenty, G., 2005. Unique coexpression in osteoblasts of broadly expressed genes accounts for the spatial restriction of ECM mineralization to bone. Genes Dev. 19 (9), 1093–1104.
Nair, A.K., Gautieri, A., Chang, S.-W., Buehler, M.J., 2013. Molecular mechanics of mineralized collagen fibrils in bone. Nat. Commun. 4, 1–9.
Oldknow, K.J., MacRae, V.E., Farquharson, C., 2015. Endocrine role of bone: recent and emerging perspectives beyond osteocalcin. J. Endocrinol. 225 (1), R1–R19.
Orgel, J.P., Eid, A., Antipova, O., Bella, J., Scott, J.E., 2009. Decorin core protein (decoron) shape complements collagen fibril surface structure and mediates its binding. PLoS One 4 (9), e7028.
Orgel, J., San Antonio, J., Antipova, O., 2011. Molecular and structural mapping of collagen fibril interactions. Connect. Tissue Res. 52 (1), 2–17.
O'Young, J., Liao, Y., Xiao, Y., Jalkanen, J., Lajoie, G., Karttunen, M., Goldberg, H.A., Hunter, G.K., 2011. Matrix Gla protein inhibits ectopic calcification by a direct interaction with hydroxyapatite crystals. J. Am. Chem. Soc. 133 (45), 18406–18412.
Pampena, D.A., Robertson, K.A., Litvinova, O., Lajoie, G., Goldberg, H.A., Hunter, G.K., 2004. Inhibition of hydroxyapatite formation by osteopontin phosphopeptides. Biochem. J. 378 (3), 1083–1087.
Price, P.A., Williamson, M.K., 1985. Primary structure of bovine matrix Gla protein, a new vitamin K-dependent bone protein. J. Biol. Chem. 260 (28), 14971–14975.
Price, P.A., Urist, M.R., Otawara, Y., 1983. Matrix Gla protein, a new γ-carboxyglutamic acid-containing protein which is associated with the organic matrix of bone. Biochem. Biophys. Res. Commun. 117 (3), 765–771.
Prince, C.W., Oosawa, T., Butler, W., Tomana, M., Bhown, A., Bhown, M., Schrohenloher, R., 1987. Isolation, characterization, and biosynthesis of a phosphorylated glycoprotein from rat bone. J. Biol. Chem. 262 (6), 2900–2907.
Ramamurthy, P., Hocking, A.M., McQuillan, D.J., 1996. Recombinant decorin glycoforms purification and structure. J. Biol. Chem. 271 (32), 19578–19584.

Reed, C.C., Iozzo, R.V., 2002. The role of decorin in collagen fibrillogenesis and skin homeostasis. Glycoconj. J. 19 (4–5), 249–255.
Rittling, S.R., Feng, F., 1998. Detection of mouse osteopontin by western blotting. Biochem. Biophys. Res. Commun. 250 (2), 287–292.
Robbiani, D.F., Colon, K., Ely, S., Ely, S., Chesi, M., Bergsagel, P.L., 2007. Osteopontin dysregulation and lytic bone lesions in multiple myeloma. Hematol. Oncol. 25 (1), 16–20.
F. Ryuichi, K. Yoshinori, Preferential adsorption of dentin and bone acidic proteins on the (100) face of hydroxyapatite crystals, Biochimica et Biophysica Acta (BBA) - General Subjects 1075(1) (1991) 56–60.
Schaefer, L., Iozzo, R.V., 2008. Biological functions of the small leucine-rich proteoglycans: from genetics to signal transduction. J. Biol. Chem. 283 (31), 21305–21309.
Schinke, T., McKee, M.D., Karsenty, G., 1999. Extracellular matrix calcification: where is the action? Nat. Genet. 21 (2), 150–151.
Schlieper, G., Westenfeld, R., Brandenburg, V., Ketteler, M., 2007. Vascular Calcification in Patients With Kidney Disease: Inhibitors of Calcification in Blood and Urine. Seminars in Dialysis, Wiley Online Library, pp. 113–121.
Scott, J.E., 1996. Proteodermatan and proteokeratan sulfate (decorin, lumican/fibromodulin) proteins are horseshoe shaped. Implications for their interactions with collagen, Biochemistry 35 (27), 8795–8799.
Scott, J.E., Orford, C.R., 1981. Dermatan sulphate-rich proteoglycan associates with rat tail-tendon collagen at the d band in the gap region. Biochem. J. 197 (1), 213–216.
Scott, J.E., Orford, C.R., Hughes, E.W., 1981. Proteoglycan-collagen arrangements in developing rat tail tendon. An electron microscopical and biochemical investigation, Biochemical Journal 195 (3), 573–581.
Scott, P.G., McEwan, P.A., Dodd, C.M., Bergmann, E.M., Bishop, P.N., Bella, J., 2004. Crystal structure of the dimeric protein core of decorin, the archetypal small leucine-rich repeat proteoglycan. Proc. Natl. Acad. Sci. U. S. A. 101 (44), 15633–15638.
Sfiridaki, A., Miyakis, S., Pappa, C., Tsirakis, G., Alegakis, A., Kotsis, V., Stathopoulos, E., Alexandrakis, M., 2011. Circulating osteopontin: a dual marker of bone destruction and angiogenesis in patients with multiple myeloma. J. Hematol. Oncol. 4 (22), 1–3.
Silva, J.C., Gorenstein, M.V., Li, G.-Z., Vissers, J.P., Geromanos, S.J., 2006. Absolute quantification of proteins by LCMSE: a virtue of parallel MS acquisition. Mol. Cell. Proteomics 5 (1), 144–156.
Silver, F.H., Freeman, J.W., Horvath, I., Landis, W.J., 2001. Molecular basis for elastic energy storage in mineralized tendon. Biomacromolecules 2 (3), 750–756.
Sodek, J., Ganss, B., McKee, M., 2000. Osteopontin. Crit. Rev. Oral Biol. Medicine 11 (3), 279–303.
Staines, K.A., MacRae, V.E., Farquharson, C., 2012. The importance of the SIBLING family of proteins on skeletal mineralisation and bone remodelling. J. Endocrinol. 214 (3), 241–255.
Stubbs, J.T., Mintz, K.P., Eanes, E.D., Torchia, D.A., Fisher, L.W., 1997. Characterization of native and recombinant bone sialoprotein: delineation of the mineral-binding and cell adhesion domains and structural analysis of the RGD domain. J. Bone Miner. Res. 12 (8), 1210–1222.
J. Termine, A. Belcourt, P. Christner, K. Conn, M. Nylen, Properties of dissociatively extracted fetal tooth matrix proteins. I. Principal molecular species in developing bovine enamel, J. Biol. Chem. 255(20) (1980) 9760–9768.
Thorpe, C.T., Birch, H.L., Clegg, P.D., Screen, H.R., 2013. The role of the non-collagenous matrix in tendon function. Int. J. Exp. Pathol. 94 (4), 248–259.
Wang, Z., Ustriyana, P., Chen, K., Zhao, W., Xu, Z., Sahai, N., 2020. Toward the understanding of small protein-mediated collagen intrafibrillar mineralization. ACS Biomaterials Science & Engineering 6 (7), 4247–4255.
Wei, J., Karsenty, G., 2015. An overview of the metabolic functions of osteocalcin. Rev. Endocr. Metab. Disord. 16 (2), 93–98.
Weiner, S., Dove, P.M., 2003. An overview of biomineralization processes and the problem of the vital effect. Rev. Mineral. 54 (1), 1–29.
Wennberg, C., Hessle, L., Lundberg, P., Mauro, S., Narisawa, S., Lerner, U.H., Millán, J.L., 2000. Functional characterization of osteoblasts and osteoclasts from alkaline phosphatase knockout mice. J. Bone Miner. Res. 15 (10), 1879–1888.
Yuan, Q., Jiang, Y., Zhao, X., Sato, T., Densmore, M., Schuler, C., Erben, R.G., McKee, M. D., Lanske, B., 2014. Increased osteopontin contributes to inhibition of bone mineralization in FGF23-deficient mice. J. Bone Miner. Res. 29 (3), 693–704.
Zhang, W., Liao, S., Cui, F., 2003. Hierarchical self-assembly of nano-fibrils in mineralized collagen. Chem. Mater. 15 (16), 3221–3226.
Zhang, J., Xin, L., Shan, B., Chen, W., Xie, M., Yuen, D., Zhang, W., Zhang, Z., Lajoie, G. A., Ma, B., 2012. PEAKS DB: de novo sequencing assisted database search for sensitive and accurate peptide identification. Mol. Cell. Proteomics 11 (4), M111–010587.
Zhao, W., Wang, Z., Xu, Z., Sahai, N., 2018. Osteocalcin facilitates calcium phosphate ion complex growth as revealed by free energy calculation. Phys. Chem. Chem. Phys. 20 (18), 13047–13056.
Zhu, X.-L., Ganss, B., Goldberg, H.A., Sodek, J., 2001. Synthesis and processing of bone sialoproteins during de novo bone formation in vitro. Biochem. Cell Biol. 79 (6), 737–746.
Zoch, M.L., Clemens, T.L., Riddle, R.C., 2016. New insights into the biology of osteocalcin. Bone 82, 42–49.